arXiv:1103.4932v1 [cond-mat.other] 25 Mar 2011

Equilibrium rotation of a vortex bundle terminating on a lateral wall

E. B. Sonin[1] and S. K. Nemirovskii[2]

[1] *Racah Institute of Physics, Hebrew University of Jerusalem, Jerusalem 91904, Israel*

[2] *Institute of Thermophysics, Prospect Lavrentyeva, 1, 630090, Novosibirsk, Russia*

(Dated: January 18, 2013)

Abstract

The paper investigates possibility of equilibrium solid-body rotation of a vortex bundle diverging at some height from a cylinder axis and terminating on a lateral wall of a container. Such a bundle arises when vorticity expands up from a container bottom eventually filling the whole container. The analysis starts from a single vortex, then goes to a vortex sheet, and finally addresses a multi-layered crystal vortex bundle. The equilibrium solid-body rotation of the vortex bundle requires that the thermodynamic potentials in the vortex-filled and in the vortex-free parts of the container are equal providing the absence of a force on the vortex front separating the two parts. The paper considers also a weakly non-equilibrium state when the bundle and the container rotate with different angular velocities and the vortex front propagates with the velocity determined by friction between vortices and the container or the normal liquid moving together with the container.

PACS numbers: 67.30.hb,47.15.ki, 67.30.he

I. INTRODUCTION

Transient processes of establishing of stable vorticity in rotating superfluids have always been in the focus of attention of theorists and experimentalists studying superfluid vortex dynamics. An important example of such a process is penetration of a vortex bundle into an originally vortex-free rotating container filled with a superfluid. This process was thoroughly investigated in superfluid ^{3}He-B theoretically and experimentally[1–3]. Vorticity is generated at the container bottom and propagates upward along the cylindric container axis in the form of a vortex bundle flaring to lateral container walls. The flaring part of the vortex bundle was called *vortex front*. Below the front the vortex bundle is vertical but twisted. The twist is connected with the flux of the angular momentum along the bundle, which must dissipate due to either mutual friction in the bulk or friction at rough wall surface. A great attention was directed to transition from laminar to turbulent vortex front propagation, especially at low temperature where disappearance of mutual friction facilitates the transition to turbulence.

All studies of the flaring vortex bundle, analytical, numerical, and experimental, were performed in the presence of dissipation, without which front propagation is impossible since it is accompanied by change of the total energy and the angular momentum. The goal of the present work was to check whether a stable solution for a vortex bundle terminating on a lateral wall may exist as an equilibrium state without dissipation and propagation along the rotation axis. In this equilibrium state the whole bundle together with its vortex front rotates without twisting as a solid with constant angular velocity. If the container rotates with the same angular velocity neither dissipation nor propagation of the vortex front along the rotation axis is possible. Our paper considers conditions for existence of such "eigenrotation" and analyses the effect of weak friction, which leads to propagation of the vortex front if the container and the bundle rotate with different angular velocities.

The paper starts from the predecessor of the vortex bundle: a single vortex filament, located on the container axis in the lower part of the container, at its higher part continuously goes away from the axis and eventually terminates on the lateral wall (Sec. II). Section III analyses a vortex bundle in which vortices form a single axisymmetric layer (vortex sheet). Section IV addresses the case of two coaxial non-interacting sheets and demonstrates that it is impossible to find the equilibrium solid-body rotation for such a two-layer bundle. This led to conclusion that equilibrium solid-body rotation of a multi-layered vortex bundle

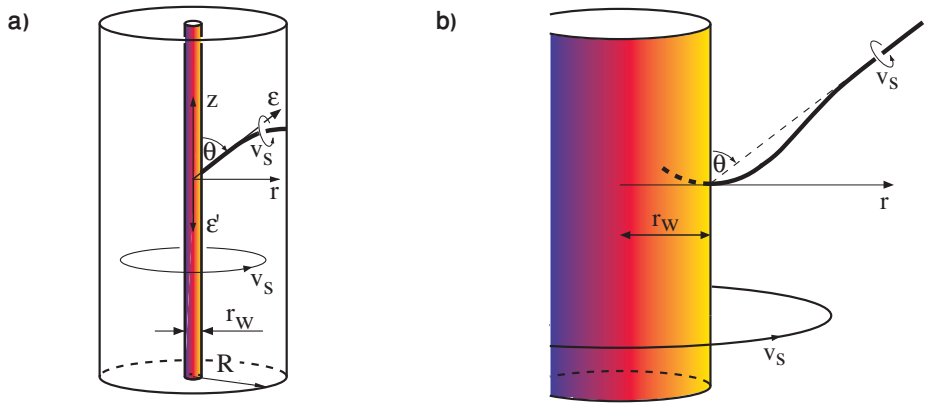

FIG. 1. (Color online) Vortex line attached to a thin wire.The profile of the vortex line can be examined on two different length scales: (a) At large scales $r \gg r_w$ the local induction approximation becomes applicable, in which the wire is treated as an enhanced vortex core. The vortex line meets a wire at the finite contact angle θ. (b) On small scales $r \sim r_w$ the vortex line goes smoothly over into the image vortex (dashed continuation of the vortex line), with the wire surface perpendicular at the connection point.

requires effective interaction between layers. This could be the same interaction, which leads to formation of a vortex crystal. The condition of equilibrium rotation of a stiff solid-body vortex bundle diverging to a lateral wall at some height is analyzed in Sec. V. Section VI discusses weakly non-equilibrium vortex bundle, when friction of the rotating vortex bundle makes possible propagation of the vortex front along the rotation axis. Concluding remarks are presented in the last Sec. VII.

II. SINGLE VORTEX

Let us start from the most elementary case when the bundle reduces to a single vortex, which terminates on a lateral wall of a container. A freely precessing vortex is in fact a particular case of the geometry, which has already been carefully investigated theoretically and experimentally in connection with the study of precession of single vortex trapped on a wire coaxial with a cylindric container filled by superfluid ^{3}He-B[4–8]. Geometry of the experiment[4] is shown in Fig. 1(a). The z-axis is the axis of the cell of the radius R and of the wire of the radius r_w. The vortex filament with the circulation κ of the superfluid velocity being trapped on the wire at $z < z_0$, peels from the wire at $z = z_0$ stretching to

the container lateral wall. Just the "unzipped" (free) part of the vortex filament at $z > z_0$ participates in the precession.

If dissipation is absent, the vortex-line shape may be found by minimization of the energy in the coordinate frame rotating with the angular velocity Ω of the vortex precession. This energy corresponds to the Gibbs thermodynamic potential

$$G = E - \Omega M_z, \tag{1}$$

where

$$E = z_0 \frac{\rho_s \kappa^2}{4\pi} \ln \frac{R}{r_w} + + \int_{r_w}^{R} \frac{\rho_s \kappa^2}{4\pi} \ln \frac{R}{r_c} \sqrt{1 + \left[\frac{dz(r)}{dr}\right]^2}\, dr \tag{2}$$

is the energy in the local induction approximation,

$$M_z = \frac{\rho_s \kappa}{2}(R^2 - r_w^2) z_0 + \rho_s \kappa \int_{r_w}^{R} [z(r) - z_0] r dr \tag{3}$$

is the angular momentum of the liquid around the axis z, r_c is the vortex core radius, and the shape of the vortex line in the cylindric coordinates is given by the function $z(r)$. It is supposed that the line is inside the axial plane, so the azimuthal angle ϕ does not vary along the line. The function $z(r)$ is determined by variation of the thermodynamic potential with respect to the vertical coordinate z of the vortex line. The corresponding Euler–Lagrange equation is

$$\rho_s \kappa \Omega r = -\frac{d}{dr}\left[\frac{\varepsilon(r)\, dz/dr}{\sqrt{1 + (dz/dr)^2}}\right], \tag{4}$$

where

$$\varepsilon = \frac{\rho_s \kappa^2}{4\pi} \ln \frac{R}{r_c} \tag{5}$$

is the energy per unit length of the vortex line, which determines the line-tension force. Equation (4) was derived from minimization of the thermodynamic potential, but at the same time it is the equation of balance of forces on the precessing vortex line: the Magnus force on the left-hand side, which is determined by the linear velocity Ωr of the precession, is balanced by the line tension force $\propto \varepsilon$. One should look for a solution of this equation with the boundary conditions on the lateral wall and the wire. The first one is the condition of transversality (the vortex line normally ends at the lateral wall of the cylinder):

$$\left.\frac{dz}{dr}\right|_{r=R} = 0. \tag{6}$$

The second boundary condition is imposed in the "unzipping" point $z = z_0$:

$$\cos\theta = \left[\frac{dz/dr}{\sqrt{1+(dz/dr)^2}}\right]\Bigg|_{r=r_w} = \frac{\varepsilon}{\varepsilon_w} = \frac{\ln\frac{R}{r_w}}{\ln\frac{R}{r_c}}, \tag{7}$$

where θ is the angle between the z axis and the vortex line at $z = z_0$ and $\varepsilon_w = (\rho_s\kappa^2/4\pi)\ln(R/r_w)$ is the line tension of the vortex filament attached to the wire. The condition directly follows from minimization of the Gibbs potential with respect to variation of the unzipping coordinate z_0[7]. It ensures the balance of line-tension forces along the z axis for the element of the vortex filament in the point $z = z_0$ (see Fig. 1): The unzipping point is at rest if $\varepsilon_w = \varepsilon\cos\theta$. In our approach the trapped segment of the vortex line is treated as a vortex line with a larger core radius r_w. So the approach is valid only for rather thin wires with radius r_w much less than the radius R of the container.

Integrating Eq. (4) over r with the transversality condition Eq. (6) one obtains the first integral

$$\frac{\rho_s\kappa}{2}\Omega(r^2 - r_w^2) = \frac{\rho_s\kappa^2}{4\pi}\ln\frac{R}{r_c}\left[\frac{dz/dr}{\sqrt{1+(dz/dr)^2}}\right]. \tag{8}$$

At the unzipping point this equation together with boundary condition Eq. (7) yields that

$$g = e - \Omega m_z = 0, \tag{9}$$

where g, $e = \varepsilon_w$, and $m_z = \rho_s\kappa\Omega(r^2 - r_w^2)/2$ are the Gibbs potential, the energy and the angular momentum per unit length of the vortex line below the unzipping point. Emergence of the condition of zero Gibbs potential below the unzipping point from the minimization of the total Gibbs potential is quite natural. In the vortex-free region the Gibbs potential density vanishes, and if the Gibbs potential density below the unzipping point is nonzero, then there is a force driving the curved piece of the vortex line (an analog of the vortex front) upward or downward. The condition (9) determines the precession angular velocity of the curved vortex line stretched between the wire and the cell lateral wall[4]:

$$\Omega = \frac{\kappa}{2\pi(R^2 - r_w^2)}\ln\frac{R}{r_w} \approx \frac{\kappa}{2\pi R^2}\ln\frac{R}{r_w}. \tag{10}$$

Note that this expression is exact and does not depend on vortex line shape of the curved segment or on using the local induction approximation[4–7]. This is a direct consequence of the rigorous canonic relation

$$\Omega = \frac{\partial E}{\partial M_z}. \tag{11}$$

Varying the position of the unzipping point the variations of the energy and momentum are $dE = \varepsilon_w dz_0$ and $dM_z = m_z dz_0$, so $\partial E/\partial M_z = \varepsilon_w/m_z$, and Eq. (11) yields expression Eq. (10) for the precession angular frequency.

This analysis can be applied to the case of a free axial vortex ending at the wall. The case is the limit of an extremely thin wire when the wire radius must be replaced by the vortex core radius in all expression. Formally this means that the unzipping point goes to $z \to -\infty$, and the curved vortex line smoothly approaches to the vertical axis of rotation in accordance with the boundary condition Eq. (7), which now tells that

$$\left.\frac{dz}{dr}\right|_{r=0} \to \infty. \tag{12}$$

The shape of the free vortex can be analytically obtained after the second integration of Eq. (8) taking into account the expression Eq. (10) for the angular velocity Ω:

$$z(r) = \sqrt{2R^2 - r^2} - R - \frac{R}{\sqrt{2}} \ln \frac{R\sqrt{2} + \sqrt{2R^2 - r^2}}{r(\sqrt{2}+1)}. \tag{13}$$

The expression demonstrates that the vortex line exponentially approaches to the axis $r = 0$: $r \approx Re^{-|z|\sqrt{2}/R}$.

While the frequency of the single vortex precession straightforwardly follows from commonly accepted thermodynamic arguments, the shape of the vortex line was a matter of dispute resulting from disagreement on a proper usage of the local induction approximation for the precessing partially trapped vortex line. One may find a detailed discussion of the issue in Refs. 7 and 8. In particular, the debate was about a proper boundary condition at the unzipping point. Instead of the boundary condition Eq. (7) based on the balance of forces directly following from the variational principle Schwarz[6] used the condition that the vortex line is normal to the wire. At the very surface of the wire the latter boundary condition is definitely correct. But at small scales of the order of the wire radius r_w there are forces, which led to fast deviation from the normal direction. These forces were neglected by Schwarz and all others addressing this problem. This is a legitimate approximation when one looks for the vortex shape at large scales of the order of the container radius R but only if one uses the boundary condition (7) based on the balance of line-tension forces. In reality this means that the boundary condition is imposed not exactly at the radius r_w of the wire but on the distance larger than r_w, which at the same time is still much smaller than R, as illustrated in Fig. 1b. It is worthwhile to note that the analysis of the shape of a

free precessing vortex gives one more justification of the force-balance boundary condition. The latter provides a natural transition from the vortex partially trapped by the wire to a free vortex smoothly changing its direction from vertical to horizontal. On the other hand, Schwarz's boundary condition becomes senseless for the free vortex since it requires that the vortex meets the axis normally.

III. SINGLE VORTEX SHEET

Our next step is to analyze a bundle of vortices but still of simple geometry: N_1 vortices form a cylindric vertical sheet of radius r_1 which at some height diverges to lateral wall forming a whorl (see Fig. 2). The single-sheet whorl is a simulation of a more complicated vortex front. As in the case of a single vortex, any vortex line in the sheet is given by the function $z(r)$, which is independent on ϕ and is determined from the variational principle for the the total Gibbs potential $G = E - \Omega M_z$. The total angular momentum is

$$M_z = \rho_s \int_{r_1}^{R} 2\pi r dr \int^{z(r)} dz[v_s(r)r] = \rho_s N_1 \kappa \int_{r_1}^{R} z(r) r \, dr, \tag{14}$$

where $v_s(r) = N_1\kappa/2\pi r$ is the azimuthal superfluid velocity induced by the vortex sheet. The total kinetic energy $E = E_s + E_v$ consists of the energy

$$E_s = \rho_s \int_{r_1}^{R} 2\pi r dr \int^{z(r)} dz \frac{v_s(r)^2}{2} = \frac{\rho_s (N_1\kappa)^2}{4\pi} \int_{r_1}^{R} z(r) \frac{dr}{r} \tag{15}$$

of the velocity field induced by the vortex sheet and the energy of individual vortex lines given by [compare with the expression Eq. (2) for a single vortex]:

$$E_v = \frac{\rho_s N_1 \kappa^2}{4\pi} \int_{r_1}^{R} \ln \frac{b}{r_c} \sqrt{1 + \left[\frac{dz(r)}{dr}\right]^2} \, dr, \tag{16}$$

where $b = 2\pi r/N_1$ the r-dependent intervortex spacing.

Variation of the Gibbs potential of the vortex sheet yields the Euler–Lagrange equation:

$$\rho_s N_1 \kappa \Omega r - \frac{\rho_s (N_1\kappa)^2}{4\pi} \frac{1}{r} = \frac{N_1 \rho_s \kappa^2}{4\pi} \frac{d}{dr} \ln\left(\frac{2\pi r}{N_1 r_c}\right) \frac{dz/dr}{\sqrt{1 + (dz/dr)^2}}. \tag{17}$$

The first integral of this equation for the boundary condition Eq. (6) at the container lateral wall is

$$\frac{\rho_s N_1 \kappa \Omega}{2} \left(r^2 - R^2\right) - \frac{\rho_s (N_1\kappa)^2}{4\pi} \ln\left(\frac{r}{R}\right) + \frac{N \rho_s \kappa^2}{4\pi} \ln\left(\frac{2\pi r}{N_1 r_c}\right) \frac{dz/dr}{\sqrt{1 + (dz/dr)^2}} = 0. \tag{18}$$

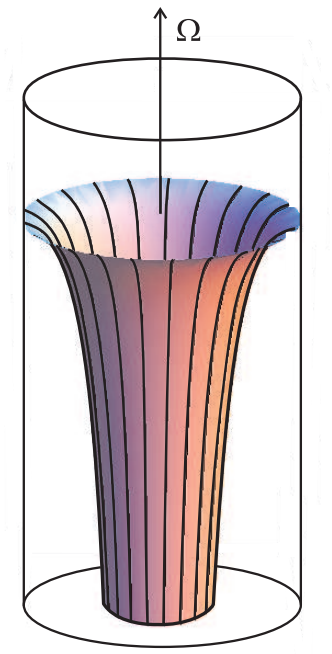

FIG. 2. (Color online) Single vortex sheet diverging to lateral walls via forming a whorl

The boundary condition

$$\left.\frac{dz}{dr}\right|_{r=r_1} \to \infty \tag{19}$$

provides a transition from the whorl to the vertical stem of the vortex sheet. Using it in Eq. (18) gives the condition that the Gibbs potential per unit length $g_1 = \varepsilon - \Omega m_z$ (ε and m_z are the energy and the angular momentum per unit length of the stem) vanishes at the stem:

$$g_1 = \frac{\rho_s (N_1\kappa)^2}{4\pi} \ln\left(\frac{R}{r_1}\right) + \frac{N_1\rho_s\kappa^2}{4\pi} \ln\left(\frac{2\pi r_1}{N_1 r_c}\right) - \frac{\rho_s N_1 \kappa\Omega}{2}\left(R^2 - r_1^2\right) = 0. \tag{20}$$

As in the case of a single vortex, this condition is necessary for the absence of the force driving the front along the vertical axis.

But our minimization of the Gibbs potential requires an additional step: minimization g with respect to r_1 at fixed number N of vortices. The minimization yields that

$$\Omega = \frac{(N_1 - 1)\kappa}{4\pi r_1^2}. \tag{21}$$

The relation means that the whole sheet rotates as a solid body with linear velocity $\Omega r_1 = (N_1 - 1)\kappa/4\pi r_1$. Though our analysis was based on the local induction approximation, for the vertical part (stem) of the vortex sheet the obtained expression is exact and is easily derived

from the Bio–Savart law for N_1 equidistant vortices on the circumference of the radius r_1. The modulus of the velocity induced by one vortex on another, $v_{ind} = \kappa/2\pi\delta$, is determined by the distance $\delta = 2r_1 \sin(\alpha/2)$ between them, where α is the angle between radii directed from the center to the both vortices. The azimuthal component $v_{ind} \sin(\alpha/2) = \kappa/4\pi r_1$ of the velocity does not depend on distance between two vortices, and therefore any vortex in the sheet moves along the circumference with the azimuthal velocity $v_{sheet} = (N-1)\kappa/4\pi r_1$ induced by rest $N-1$ vortices. The radial component of any vortex vanishes for equidistant location of vortices by symmetry. If $N_1 \gg 1$ the velocity $v_{sheet} = 1/2\,(v_{in} + v_{out})$ is an average of the velocities $v_{in} = 0$ and $v_{out} = N_1\kappa/2\pi r_1$ on both sides of the sheet (inside and outside). This law of motion for vortex sheets is well known in classical hydrodynamics.

In Fig. 3 we depicted the solution of the Euler–Lagrange equation (17) with the boundary conditions $z(R) = 0$ and $dz/dr|_R = 0$ for $N_1 = 10$ and $\Omega R^2/\kappa = 4.52828$. The whorl smoothly diverges from the vertical stem with the radius determined from Eq. (21) and terminates on the lateral wall.

IV. TWO VORTEX SHEETS

One might think that a more realistic vortex bundle could be modeled as an ensemble of coaxial vortex sheets with their stems rotating together with the same angular velocity as a solid body. In order to check this option we considered two coaxial vortex sheets with numbers of vortices N_1 and N_2 diverging to lateral walls via two whorls (Fig. 4). The analysis of the Gibbs potential of the sheets below the whorls has shown that the condition for solid body rotation of the two sheets with the same angular velocity cannot be realized. The density of the Gibbs potential for two vertical sheet is $g = g_1 + g_2$ where the Gibbs

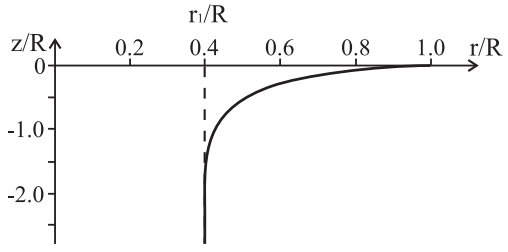

FIG. 3. The profile of the vortex sheet calculated from the Euler–Lagrange equation (17) for $N_1 = 10$ and $\Omega R^2/\kappa = 4.52828$.

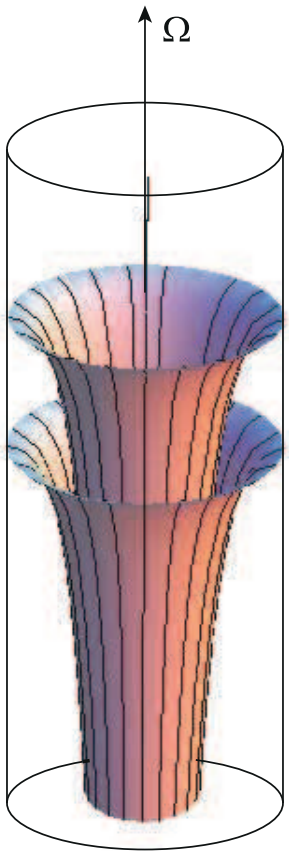

FIG. 4. (Color online) Hypothetical picture of two vortex sheets terminating on the lateral wall. But no state of solid-body rotation of two sheets with the same angular velocity was found.

potential g_1 per unit length of the inner sheet is given by Eq. (20) and the Gibbs potential g_2 per unit length of the outer sheet is

$$g_2 = \frac{\rho_s \kappa^2 N_2(2N_1 + N_2)}{4\pi} \ln\left(\frac{R}{r_2}\right) + \frac{N_2 \rho_s \kappa^2}{4\pi} \ln\left(\frac{2\pi r_2}{N_2 a_0}\right) - \Omega \frac{\rho_s N_2 \kappa}{2} \left(R^2 - r_2^2\right). \tag{22}$$

Minimization with respect to r_2 yields the relation

$$\Omega = \frac{(N_2 + 2N_1 - 1)\kappa}{4\pi r_2^2}. \tag{23}$$

The equilibrium condition (absence of the driving force on the whorl) is satisfied only if $g_1 = 0$ and $g_2 = 0$. One may find the states with vanishing g_1 and g_2 only if the angular velocities Ω in Eqs. (21) and (23) are different. The state with the solid body rotation of two sheets together cannot be found. However this outcome results from shortcoming of our model and does not mean that the solid-body "stem + whorl" structure for multi-layer vortex bundles

is impossible. In our model the vortex sheet induces a fully axisymmetric velocity field outside the sheet and no field inside. Though discrete vortex structure of the sheet is taken into account via a logarithm contribution in the energy, the effect of individual vortices on the velocity field is neglected. Such an approximation is valid only if the distance between sheets exceeds the intervortex distance in any sheet. In a tightly packed vortex bundle the approximation fails, and interaction between neighboring layers glues them effectively and does not allow rotation with different velocities. Then the condition for an equilibrium vortex front becomes much less severe: it is not necessary for the Gibbs potential of *any* sheet to vanish, it is sufficient that the *total* Gibbs potential vanishes. The latter condition will be considered in the next section.

V. EQUILIBRIUM ROTATION OF THE SOLID-BODY VORTEX BUNDLE TERMINATING ON THE LATERAL WALL

From the analysis of a single and two vortex sheets it is evident that the most restrictive condition for equilibrium solid-body rotation of a vortex bundle terminating on the lateral wall is zero Gibbs potential much below the front. If this condition is satisfied the solution of the differential Euler–Lagrange equation for the front shape is straightforward, though technically complicated: for a multilayered vortex whorl one should solve a partial differential equation in the space of two coordinates r and z. This section addresses only the condition of solvability of this equation: absence of a force on the vortex front.

We look for the equilibrium state of fixed number N of vortices forming the solid-body vortex bundle terminating on the lateral wall and rotating with the angular velocity Ω (Fig. 5). The azimuthal velocity field in the stem of the bundle is

$$v = \begin{cases} \Omega r & r < R_0 \\ \frac{\Omega R_0^2}{r} & r > R_0 \end{cases}, \tag{24}$$

where R_0 is the radius of the bundle stem. The number of vortices and the bundle radius are connected with the relation $N = 2\pi\Omega R_0^2/\kappa$. The Gibbs potential for the unit length of the bundle stem in the coordinate frame rotating with the angular velocity Ω_0 is

$$g = \varepsilon - \Omega_0 m_z = \pi\rho_s\Omega^2 R_0^4 \left(\ln\frac{R}{R_0} + \frac{1}{4}\right) + \frac{\rho_s\kappa\Omega R_0^2}{2}\ln\frac{r_v}{r_c} - \Omega_0\pi\rho_s\Omega R_0^2\left(R^2 - \frac{R_0^2}{2}\right). \tag{25}$$

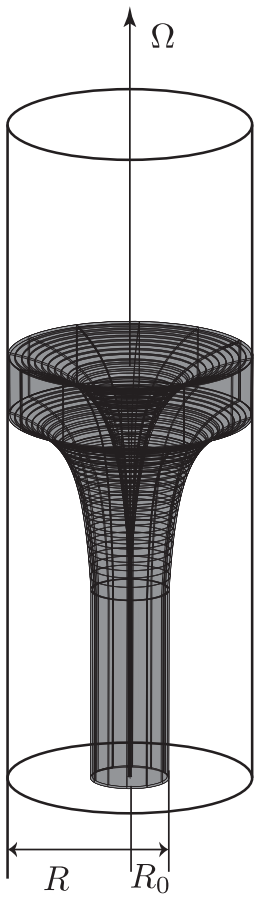

FIG. 5. (Color online) Solid-body vortex bundle terminating on the lateral wall.

In the equilibrium Ω must coincide with Ω_0 and using the relation between Ω and R_0 this equation reduces to

$$g = \frac{\rho_s \kappa^2}{4\pi}\left[N(N-1)\ln\frac{R}{R_0} + \frac{3}{4}N^2 + N\ln\frac{R}{r_c\sqrt{N}} - \frac{R^2}{R_0^2}N^2\right]. \tag{26}$$

The condition $g = 0$ yields the relation

$$\ln\frac{R}{r_c} = N\left(\frac{R^2}{R_0^2} - \frac{3}{4}\right) - (N-1)\ln\frac{R}{R_0} + \ln\sqrt{N}. \tag{27}$$

If the bundle nearly fills the whole container ($R_0 \approx R$, i.e., the number N of vortices is close to the equilibrium value)

$$\ln\frac{R}{r_c} \approx \frac{N}{4} + \ln\sqrt{N}. \tag{28}$$

So the condition for equilibrium rotation of the bundle terminating on the lateral wall can be satisfied but not for a very large number of vortices. If the filling factor R_0/R is small, unrealistically high values of $\ln(R/r_c)$ are required for equilibrium rotation of a large number

of vortices. Equilibrium rotation is impossible in the classical limit of continuous vorticity neglecting the vortex line tension $\propto \kappa \ln(r_v/r_c)$.

VI. NON-EQUILIBRIUM ROTATION AND FRICTION

The equilibrium finite vortex bundle may rotate freely only if a container rotates with the same angular velocity or there is no friction force between moving vortices and the container and the normal liquid rotating with it. In the experiment this condition is not satisfied, and dynamics and structure of the bundle require a more complicated analysis in general. But if friction is rather weak as expected in the low-temperature limit, one may consider the friction effect assuming that the structure of the vortex front (whorl) is not affected seriously.

For the state close to the equilibrium one may use the thermodynamic approach. If the vortex front moves with the velocity v_f variation of the energy of the vortex bundle rotating with the angular velocity Ω during a short time interval dt is (the energy of the front is neglected compared to that of the bundle stem)

$$dE_b = e(\Omega) v_f dt. \tag{29}$$

Displacement of the vortex front is accompanied by variation of the bundle angular momentum $dM_z = m_z v_f dt$. The total angular momentum is conserved, and the angular momentum dM_z must be transferred from the container via mutual friction with the normal liquid moving rigidly with the container or via surface friction of vortex ends at a rough wall. This leads to energy variation of the container rotating with the angular velocity Ω_0:

$$dE_c = \Omega_0 dM_z. \tag{30}$$

The total decrease of the energy due to front motion is

$$dE = dE_c - dE_b = -[e(\Omega) - \Omega_0 m_z(\Omega)] v_f dt. \tag{31}$$

This supports the condition of the equilibrium at $\Omega = \Omega_0$ used above: the Gibbs potential density $g(\Omega) = e(\Omega) - \Omega m_z(\Omega)$ must vanish. The quantity $F_f = e(\Omega) - \Omega_0 m_z(\Omega)$ can be interpreted as a force driving the vortex front in a non-equilibrium state. Since the total energy cannot change the released energy dE is compensated by dissipation with the rate

$\dot{Q} = dE/dt = F_f v_f$. Eltsov *et al.*[3] estimated the dissipation rate $\dot{Q}$ assuming that the bundle with $R_0 \approx R$ rotates with the same velocity as the container ($\Omega = \Omega_0$) and neglecting the quantum line-tension contribution $\propto \kappa \ln(r_v/r_c)$ to the energy. This yielded the force F_f equal to the bundle kinetic energy $\pi\rho_s\Omega^2 R^4/4$ per unit length. Here we consider the state close to the equilibrium solid-body rotation at which the force $F_f = e(\Omega) - \Omega m_z(\Omega)$ vanishes. So the force is

$$F_f = (\Omega - \Omega_0) m_z(\Omega) = \frac{\pi\rho_s(\Omega - \Omega_0)\Omega R^4}{2}. \tag{32}$$

The vortex front can move only if there is exchange of the angular momentum between the bundle and the container. We assume the phenomenological linear relation between the friction torque $t = \gamma(\Omega - \Omega_0)$ on a vortex and the relative angular velocity $\Omega - \Omega_0$. Then the balance equation for the total angular momentum of the liquid is

$$\frac{dM_z}{dt} = m_z v_f = Nt = \gamma N(\Omega - \Omega_0). \tag{33}$$

For the vortex bundle with $R_0 \approx R$ the angular momentum per unit length is $m_z = \rho_s N\kappa R^2/4$, and the front velocity

$$v_f = \frac{4\gamma(\Omega - \Omega_0)}{\rho_s \kappa R^2} \tag{34}$$

does not depend on the number of vortices in the bundle at given $\Omega - \Omega_0$.

VII. DISCUSSION AND CONCLUSIONS

The paper addressed the question whether the vortex bundle terminating on the lateral wall can rotate as a solid body and what is the angular velocity of such "eigenrotation". There are two conditions for existence of eigenrotation: (i) The whole vortex bundle including its stem and the whorl is in an equilibrium solid-body rotation with the same speed; (ii) The Gibbs potential per unit length of the stem is equal to the zero Gibbs potential of the vortex-free state above the bundle. The latter condition eventually determines the angular velocity of the eigenrotation and was used in the past for estimation of the rotation of the vortex front by Eltsov *et al.*[1,3] but without paying attention to the first condition of equilibrium solid-body rotation of the whole bundle. Indeed, using Eq. (25) for linear density g of the Gibbs potential with the filling factor $R_0/R \approx 1$ and the logarithm term $\propto \ln(r_v/r_c)$ neglected the condition $g = 0$ yields that $\Omega_0 = \Omega/2$. So in the coordinate frame

rotating with this angular velocity the Gibbs potentials above and below the vortex front are equal, and on the basis of it Eltsov *et al.* concluded that the front must rotate with the speed, which is half of the rotation speed of the container. This rotation has nothing to do with the equilibrium rotation analyzed in the present work: The vortex front rotates twice slower than the vortex bundle stem, which must leads to steady twisting of the vortex bundle. Application of thermodynamic-balance arguments to so strongly non-equilibrium state requires justification, and a more rigorous dynamical approach of the problem is wanted. The analysis of the equilibrium and weakly non-equilibrium vortex bundle presented in the present paper can be considered as the first step in this direction.

ACKNOWLEDGMENTS

The work was supported by the grant of the Israel Academy of Sciences and Humanities. One of authors (S. K. N.) thanks the Racah Institute of Physics of the Hebrew University of Jerusalem for hospitality and support and acknowledges a partial support by the grants N 10-08-00369 and N 10-02-00514 from the Russian Foundation of Basic Research.

---

[1] V. B. Eltsov, A. P. Finne, R. Hänninen, J. Kopu, M. Krusius, M. Tsubota, and E. V. Thuneberg, Phys. Rev. Lett. **96**, 215302 (2006).

[2] V. B. Eltsov, R. de Graaf, P.J. Heikkinen, J. J. Hosio, R. Hänninen, M. Krusius, and V. S. L'vov, Phys. Rev. Lett. **105**, 125301 (2010).

[3] V. B. Eltsov, R. de Graaf, J. J. Hosio, P.J. Heikkinen, R. Hänninen, M. Krusius, V. S. L'vov, and G. E. Volovik, arXiv:1102.4284.

[4] R. J. Zieve, Yu. Mukharsky, J. D. Close, J. C. Davis, and R. E. Packard, Phys. Rev. Lett. **68**, 1327 (1992).

[5] T.Sh. Misirpashaev and G.E. Volovik, Pis'ma Zh. Eksp. Teor. Fiz. **56**, 40 (1992) [JETP Lett. **56**, 41 (1992)].

[6] K.W. Schwarz, Phys. Rev B **47**, 12030 (1993).

[7] E. B. Sonin, J. Low Temp. Phys. **97**, 145 (1994).

[8] E. B. Sonin and M. Krusius, in: *Vortex State. Proceedings of the NATO Advanced Study Institute on Vortices in Superfluids* (Cargese, Corsica, 1993), eds. N. Bontempts, Y. Bruynseraede, G. Deutscher, and A. Kapitulnik (Kluver Academic Press, 1994) pp. 193-230.